BOS-93, a novel bromophenol derivative, induces apoptosis and autophagy in human A549 lung cancer cells via PI3K/Akt/mTOR and MAPK signaling pathway

CHUANLONG GUO[1,2*], LIJUN WANG[1,2*], YUE ZHAO[1,2], BO JIANG[1,2], JIAO LUO[1,2] and DAYONG SHI[1,2]

[1]CAS Key Laboratory of Experimental Marine Biology, Institute of Oceanology, Chinese Academy of Sciences; [2]Laboratory for Marine Drugs and Bioproducts of Qingdao National Laboratory for Marine Science and Technology, Qingdao, Shandong 266071, P.R. China

Received June 7, 2018; Accepted November 20, 2018

DOI: 10.3892/etm.2019.7402

Abstract. The novel bromophenol derivative, 3-(3-bromo-5-methoxy-4-(3-(piperidin-1-yl)propoxy)benzylidene)-*N*-(4-bromophenyl)-2-oxoindoline-5-sulfonamide (BOS-93), was synthesized in the CAS Key Laboratory of Experimental Marine Biology, Institute of Oceanology, Chinese Academy of Sciences (Qingdao, China). Experimental studies have demonstrated that it could induce apoptosis and autophagy in human A549 lung cancer cells, and it could also inhibit tumor growth in human A549 lung cancer xenograft models. In the present study, the molecular pathways underlying these effects were identified. The results demonstrated that BOS-93 could inhibit cell proliferation in A549 cells and block A549 cells at the G0/G1 phase. Furthermore, BOS-93 could induce apoptosis, activate caspase-3 and poly ADP ribose polymerase, and increase the B cell lymphoma (Bcl)-2 associated X protein/Bcl-2 ratio. Notably, BOS-93 could also induce autophagy in A549 cells. BOS-93-induced autophagy was confirmed by detecting light chain 3 (LC3)-I/LC3-II conversion and increasing expression of beclin1 and autophagy-related gene 14. Notably, BOS-93-induced autophagy could be inhibited by the autophagy inhibitor 3-MA. Flow cytometry, transmission electron microscopy (TEM) and western blot analysis indicated that BOS-93 induced apoptosis and autophagy activities by deactivating phosphoinositide 3-kinase/protein kinase B/mechanistic target of rapamycin and activating the mitogen-activated protein kinase signaling pathway. The present findings indicated that BOS-93 might be a novel anti-cancer agent for treatment of human lung cancer.

Correspondence to: Professor Dayong Shi, CAS Key Laboratory of Experimental Marine Biology, Institute of Oceanology, Chinese Academy of Sciences, 7 Nanhai Road, Qingdao, Shandong 266071, P.R. China
E-mail: shidayong@qdio.ac.cn

*Contributed equally

Key words: bromophenol, apoptosis, autophagy, phosphoinositide 3-kinase/protein kinase B/mechanistic target of rapamycin signaling, reactive oxygen species

Introduction

Bromophenols, a unique type of compound derived from marine sources, are mainly isolated from marine fungi, marine algae, sponges, ascidians, and bryozoans (1,2). It is difficult to separate natural bromophenols from marine organisms, and they often exhibit low biological activity (3-5). However, bromophenol derivatives exhibit excellent biological activity, including anti-oxidation, antibacterial and anti-tumor activities (3,4). In our previous study, a series of bromophenol compounds were designed. This series of compounds exhibited excellent anti-tumor activities and could inhibit the growth of a variety of tumor cells (6). One of these compounds, 3-(3-bromo-5-methoxy-4-(3-(piperidin-1-yl)propoxy)benzylidene)-*N*-(4-bromophenyl)-2-oxoindoline-5-sulfonamide (BOS-93; Fig. 1A), exhibited significant anti-tumor activities. Notably, in the present study, it was demonstrated to induce autophagy in A549 cells, unlike the mechanisms of the compounds we previously reported.

Apoptosis is the autonomous, orderly death of cells controlled by genes to maintain homeostasis. It mainly comprises two representative pathways: The mitochondrial pathway, which is the major pathway, and the death receptor-mediated pathway (7). Reactive oxygen species (ROS) also serve a critical role in the mitochondrial pathway; generation of ROS can induce mitochondrial membrane damage, releasing cytochrome c from injured mitochondria and thereby inducing cell apoptosis (8).

Autophagy, also known as type II cell death, is the process by which cells use lysosomes to degrade their own damaged organelles and macromolecules under the control of autophagy-related genes (Atg) (9). Apoptosis and autophagy are the molecular mechanisms by which cells maintain organelles and homeostasis. Although autophagy can also lead to cell death under certain conditions, it primarily maintains a constant state in a cell through selective reutilization of organelles and macromolecules (10,11).

Autophagy begins with the production of double-membrane vacuoles (named autophagosomes) that entrap the material to be degraded and eventually fused with lysosomes (12).

Autophagosomes are characterized by the presence of the protein light chain 3 (LC3) (derived from posttranslational modifications of a microtubule-associated protein precursor) on their membranes. Beclin-1, which was initially isolated as an interactor of the oncogenic anti-apoptotic protein among many proteins that directly or indirectly regulate the autophagy process (12,13).

In eukaryotes, autophagy is an important process that is evolutionarily reserved for turnover of intracellular material (13). The mammalian target of rapamycin (mTOR) signaling pathway, and the phosphoinositide 3-kinase (PI3K)/protein kinase B (Akt)/mTOR pathway in particular, is associated with most physiological processes, including cell metabolism, proliferation and autophagy (14,15).

In the present study, the mechanism underlying the anti-cancer effects of BOS-93 in A549 lung cells was investigated. The results demonstrated that BOS-93 could induce apoptosis and cause autophagy in A549 cells. In addition, the molecular mechanisms underlying BOS-93-induced apoptotic and autophagic death in A549 cells were investigated. Further studies indicated that the PI3K/Akt/mTOR and p38/extracellular signal-regulated kinase signaling pathways were associated with BOS-93-induced apoptosis and autophagy. In summary, the present results indicated that BOS-93 may be a promising anti-tumor drug against human lung cancers.

Materials and methods

Reagents, chemicals and antibodies. BOS-93 was synthesized by the CAS Key Laboratory of Experimental Marine Biology, Institute of Oceanology, Chinese Academy of Sciences, (Qingdao, China; purity >98%) (6). The purity of compound BOS-93 was measured by high-performnce liquid chromatography (HPLC; Shimadzu Corporation, Kyoto, Japan), carried out on a Shimadzu LC-20A system (Shimadzu Corporation) equipped with a Shimadzu InertSustain C-18 reverse phase column (4.6x250 x5 μm; Shimadzu Corporation) and SPD-20A detector (Shimadzu Corporation). HPLC was conducted at 25˚C with 70% methanol and 50% acetonitrile mobile phases. The flow rate was 1 ml/min and samples were 10 μl. The F-12K and RPMI-1640 mediums were obtained from Hyclone; GE Healthcare Life Sciences (Logan, UT, USA), fetal bovine serum (FBS) was obtained from ExCell Bio, Inc., (Shanghai, China), other culture reagents were purchased from Invitrogen; Thermo Fisher Scientific, Inc., (Waltham, MA, USA). Reactive oxygen species (ROS) assay kit, apoptosis assay kit, Hoechst 33258 staining kit and adenovirus (Ad)-green fluorescent protein (GFP)-LC3 were obtained from Beyotime Institute of Biotechnology (Haimen, China). Autophagy inhibitor 3-MA was obtained from Dalian Meilun Biotech Co., Ltd. (Dalian, China). The antibodies against cyclin D1 (Rabbit mAb, cat. no. 2978; 1:1,000), cyclin-dependent kinase (CDK)4 (Rabbit mAb cat. no. 12790; 1:1,000), cleaved-poly ADP ribose polymerase (PARP; Rabbit mAb cat. no. 9532; 1:1,000), B cell lymphoma (Bcl)-2 (Mouse mAb cat. no. 15071; 1:1,000), Bcl-2-associated X protein (Bax; Rabbit cat. no. 2774; 1:1,000), cleaved-caspase-3 (Rabbit; cat. no. 9661; 1:1,000), phosphorylated (p)-PI3K (Rabbit, cat. no. 4228; 1:1,000), PI3K (Rabbit mAb cat. no. 4257; 1:1,000), p-Akt (Rabbit mAb cat. no. 4060; 1:2,000), Akt (Mouse mAb cat. no. 2920; 1:2,000), p-p38 mitogen-activated protein kinase (MAPK; Rabbit mAb cat. no. 4511; 1:1,000), p38 MAPK (Rabbit mAb cat. no. 8690; 1:1,000), p-ERK1/2 (Rabbit mAb cat. no. 4370; 1:2,000), ERK1/2 (Mouse mAb cat. no. 4696; 1:2,000), LC3 (Rabbit mAb cat. no. 3868; western blotting, 1:1,000; immunohistochemistry, 1:3,200), beclin-1 (Rabbit mAb cat. no. 3495, 1:1,000) and Ki-67 [Rabbit mAb (IHC Specific) cat. no. 9027; 1:400] were purchased from Cell Signaling Technology, Inc. (Danvers, MA, USA). Antibodies against GAPDH (Rabbit, ab128915; 1:10,000), p-mTOR (Rabbit, ab109268; 1:5,000) and mTOR (Rabbit, ab32028; 1:5,000) were purchased from Abcam (Cambridge, UK). Antibody against Atg14 (Rabbit, WL02420; 1:1,000) was purchased from Wanleibio Co., Ltd. (Shanghai, China).

Cell line and culture. Cells (A549, 95D and NCI-H460) were purchased from Cell Bank, Chinese Academy of Sciences (Shanghai, China). A549 cells were maintained in F-12K medium, whereas 95D cells and NCI-H460 cells were maintained in RPMI-1640 medium, and all mediums were supplemented with 10% FBS, 100 U/ml penicillin and 100 μg/ml streptomycin. Cells were cultured at 37˚C in a humidified CO_2 (5%) atmosphere.

Determination of cell viability. Cell viability was determined via MTT assay. Cells in growth phase were plated into 96-well plates at a density of $3x10^3$ cells per well and incubated for 24 h. Then, cells were exposed to 0, 2.5, 5, 10 and 20 μg/ml BOS-93 for 48 h. Following treatment, cells were further incubated with MTT for 4 h. Then the formazan was dissolved by dimethyl sulfoxide and measured using a microplate reader at 490 nm. The 50% inhibitory concentration (IC_{50}) was defined as the concentration that reduced the absorbance of the untreated wells by 50% of the vehicle in the MTT assay.

Colony formation assay. A549 cells were harvested and 500 cells/well were seeded in 6-well plates and allowed to settle overnight at 37˚C. Then cells were treated with BOS-93 (0, 2.5, 5 and 10 μg/ml) at 37˚C for 10 days. Following treatment, cells were washed with PBS and fixed with 4% paraformaldehyde at room temperature for 10 min. Cells were washed with PBS and finally stained with crystal violet at room temperature for 10 min. Cells were scored under light microscopy (magnification, x100) and >50 cells clustered together were scored as colonies (16).

Apoptosis assay by flow cytometry. Apoptosis was determined by flow cytometry. Briefly, cells ($1x10^5$ cells/well) were seeded in 6-well plates and allowed to settle overnight at 37˚C, and then cells were treated with BOS-93 (0, 2.5, 5 and 10 μg/ml) for 48 h. Cells were harvested and stained with Annexin V-fluorescein isothiocyanate (FITC) and propidium iodide (PI; Beyotime Institute of Biotechnology, Haimen, China) at room temperature for 15 min, then cells were analyzed using a flow cytometer (BD FACSCalibur) and CellQuest Pro software (FACSstation 6.0; BD Biosciences, Franklin Lakes, NJ, USA).

Cell cycle analysis. Cell cycle analysis was determined by flow cytometry. Briefly, A549 cells ($1x10^5$ cells/well) were harvested and seeded in 6-well plates and allowed to settle overnight at 37˚C. Cells were treated with BOS-93 (0, 2.5, 5 and 10 μg/ml)

at 37˚C. Following 48 h treatment, cells were harvested and fixed in 7% ethanol at -20˚C overnight. Cells were washed twice with PBS and stained with PI solution containing 20 μg/ml RNaseA and 50 μg/ml PI (both Beyotime Institute of Biotechnology) at 37˚C for 30 min. Then cells were analyzed using flow cytometry and CellQuest Pro software.

Hoechst 33258 staining. The cell nucleus shape was observed by fluorescence microscopy following Hoechst 33258 staining. Briefly, cells ($1x10^5$ cells/well) were seeded in 6-well plates and allowed to settle overnight at 37˚C, and then cells were treated with BOS-93 (0, 2.5, 5 and 10 μg/ml) at 37˚C for 48 h. Following treatment, cells were stained with Hoechst dye 33258 for 5 min at room temperature and assessed by fluorescence microscopy (magnification, x400; Olympus Corporation, Tokyo, Japan).

Transmission electron microscopy. A549 cells were exposed to BOS-93 (10 μg/ml) for 48 h at 37˚C and cells were fixed in 2.5% glutaraldehyde (Shanghai Yuanye Biotechnology Co., Ltd., Shanghai, China) overnight at 4˚C and postfixed with 1% osmium tetroxide (OsO_4) and kaliumhexacyanoferrate [$K_3FE(CN)_6$] in cacodylate buffer. Subsequently, the cells were dehydrated in an alcohol series and embedded in resin overnight at room temperature. Ultrathin sections (200 nm) were collected on formvar-coated grids, counterstained with uranil acetate and lead citrate at room temperature for 10 min, and visualized with transmission electron microscopy (TEM; JEM-1200EX, JEOL Ltd., Akishima, Japan; magnification, x8,000).

Analysis of cells with GFP-LC3. To detect GFP-LC3 translocation, A549 cells ($1x10^5$ cells/ml) were grown on glass coverslips at 37˚C for 24 h and then infected with Ad-GFP-LC3 (Beyotime Institute of Biotechnology). Following overnight culture at 37˚C, cells were treated with BOS-93 (10 μg/ml) at 37˚C for 48 h. Then cells were fixed with 4% paraformaldehyde at 37˚C for 20 min and examined under a fluorescence microscope (magnification, x400).

Analysis of autoghagy with 3-MA. The autophagy inhibitor 3-MA was also used to block autophagy at the final concentration of 5 mM. Briefly, A549 cells ($1x10^5$ cells/well) in a 6-well plate were pretreated with 3-MA (5 mM) at 37˚C for 1 h, and then cells were treated with BOS-93 (0, 2.5, 5 and 10 μg/ml) at 37˚C for 48 h. Cell lysates were detected by western blotting.

Measurement of intracellular ROS. The measurement of ROS was determined by flow cytometry. A549 cells ($1x10^5$ cells/well) were harvested and seeded in 6-well plates and allowed to settle overnight at 37˚C. Cells were treated with BOS-93 (0, 2.5, 5 and 10 μg/ml) for 48 h at 37˚C. The medium was removed and cells were co-incubated with 10 μM 2',7'-dichlorofluorescein diacetate (DCFH-DA; Beyotime Institute of Biotechnology) at 37˚C for 30 min. Then cells were harvested and analyzed by flow cytometry and CellQuest Pro software.

Western blot analysis. A549 cells were harvested and seeded in 6-well plates ($1x10^5$ cells/well) and allowed to settle overnight at 37˚C. Cells were treated with BOS-93 (0, 2.5, 5 and 10 μg/ml) for 48 h at 37˚C. Proteins were harvested by RIPA buffer (Beijing Solarbio Science & Technology Co., Ltd., Beijing, China) and separated by SDS-PAGE on a 10% gel and transferred onto polyvinylidene difluoride membranes. Membranes were blocked in blocking solution (containing 5% non-fat milk) at room temperature for 1 h and subsequently probed with primary antibodies at 4˚C overnight. Following 15 min washes in TBS-Tween 20, the membranes were incubated with horseradish peroxidase (HRP)-conjugated secondary antibodies (cat. no. 7074; 1:10,000; Cell Signaling Technology, Inc.) for 1 h at room temperature. The bands were detected using an enhanced chemiluminescence system BeyoECL Plus (Beyotime Institute of Biotechnology).

In vivo tumor model. Female congenital athymic BALB/c nude (nu/nu) mice (n=12) were purchased from Model Animal Research Center Of Nanjing University (Nanjing, China). Mice were housed in a specific pathogen-free room with controlled temperature (24±2˚C), humidity (60-80%) and lighting (12 h light/dark cycle) with *ad libitum* access to water and food. All experiments with mice were approved by Institute of Oceanology, Chinese Academy of Sciences Laboratory Animal Care and Ethics Committee (Qingdao, China) in accordance with the animal care and use guidelines. Efforts were made to minimize animal suffering. All experiments were carried out using 6-8-week-old mice weighting 18-22 g. Mice were given 1 week to acclimatize to the housing conditions prior to experiments. *In vitro* cultured A549 cancer cells ($1x10^7$) were injected subcutaneously into the back of mice. When the tumor reached 150 mm^3 in volume, animals were divided randomly into two groups (n=6 each) and administered with 50 mg/kg intraperitoneal BOS-93 (dissolved in 0.5% carboxymethyl cellulose-Na) for 21 days (once a day). Tumor volumes and body weight were measured every 3 days. Tumor volumes were calculated according to the following equation: Length x $(width)^2/2$. Body weight was measured every three days and clinical symptoms were observed daily. Following treatment, mice were anaesthetized with isoflurane (inhalation anesthesia; Shanghai Yuanye Biotechnology Co., Ltd., Shanghai, China) and sacrificed by decapitation and tumor tissues were collected for immunohistochemistry, and haematoxylin and eosin (H&E) analysis.

Immunohistochemistry and H&E staining. Tumor tissues were obtained, immediately fixed in 10% neutral formaldehyde at room temperature for 24 h and later embedded in paraffin wax. The paraffin-embedded tissue sections (4 μm) were treated with heat-induced antigen retrieval buffer (pH 6.0; citrate buffer; Beyotime Institute of Biotechnology) and blocked using 5% bovine serum albumin (Beijing Solarbio Science & Technology Co., Ltd.) at room temperature for 1 h.

For immunohistochemistry, samples were then incubated with rabbit anti-Ki-67 (cat. no. 9027; 1:400) or anti-LC3B (cat. no. 12741; 1:500; Cell Signaling Technology, Inc.) antibodies overnight at 4˚C. Tissue was then incubated with Equilibrate SignalStain® Boost IHC Detection Reagent (HRP, Rabbit; cat. no. 8114; Cell Signaling Technology, Inc.) for 30 min at room temperature and developed using a DAB kit (cat. no. 8059; Cell Signaling Technology, Inc.) at room temperature for 1 min. Samples were then counterstained with

hematoxylin for 30 sec at room temperature and then observed under a light microscope (magnification, x200).

For H&E staining, samples were stained with hematoxylin for 10 min at room temperature. Samples were washed with water for 10 min at room temperature and then stained with eosin for 2 min at room temperature. Samples were observed under a light microscope (magnification, x200).

Statistical analysis. Statistical analysis was performed using GraphPad Prism 5.0 (GraphPad Software, Inc., La Jolla, CA, USA). All data are presented as mean + standard deviation. Differences were analysed with one-way analysis of variance followed by Tukey's post hoc test. The difference between the control and model groups was analysed using Student's t-test. $P<0.05$ was considered to indicate a statistically significant difference.

Results

BOS-93 inhibits cell proliferation. Cell viability was detected by MTT assay. As presented in Fig. 1B, BOS-93 had a dose-dependent inhibitory effect on three human lung cancer cells including A549, 95D and NCI-H460 cells. The IC_{50} value of BOS-93 on the three cells was 4.78±0.56, 9.99±1.81 and 6.14±0.60 μg/ml, respectively. The effect of BOS-93 on the relative colony formation ability of A549 cells was also investigated. As presented in Fig. 1C and D, the clonogenicity of A549 cells was reduced in a dose-dependent manner following exposure to BOS-93.

BOS-93 induces G0/G1 cell cycle arrest. The cell cycle progression of A549 cells was analyzed via flow cytometry. A549 cells were analyzed by flow cytometry following treatment with BOS-93 (0, 2.5, 5 and 10 μg/ml) for 48 h. As presented in Fig. 2A and B, following treatment with BOS-93, the accumulation of cells in the G0/G1 phase was increased in a dose-dependent manner. The percentage of cells in the 0, 2.5, 5 and 10 μg/ml groups at the G0/G1 phase was significantly enhanced from 47.54±10.55 to 55.02±7.8, 62.89±9.30 and 72.90±5.80%, respectively.

Western blotting was used to analyze cell cycle associated proteins. As presented in Fig. 2C, following treatment with BOS-93, protein levels of cyclin D1 and CDK4 were decreased, these data indicated that BOS-93-mediated cell cycle arrest at the G0/G1 phase may inhibit the formation of CDK/cyclin complexes via downregulation of cyclin D1 and CDK4.

BOS-93 induces A549 apoptosis. Apoptosis is a major form of cell death induced by chemotherapeutic agents (17). In the present study, A549 cells were treated with BOS-93 for 48 h. Cells were stained with Annexin-V-FITC/PI and analyzed by flow cytometry. The results indicated a dose-dependent increase in the proportion of cells in which apoptosis was induced by BOS-93. The apoptotic cell rate in the 0, 2.5, 5 and 10 μg/ml groups were increased from 10.67±1.96 to 17.66±1.72, 31.66±7.16 and 46.63±8.34%, respectively (Fig. 3A and B).

Morphological changes in A549 cells were also detected with the Hoechst 33258 staining method. Apoptotic features such as nuclear shrinkage and chromatin condensation were observed, as presented in Fig. 3C. These results demonstrated that BOS-93 could induce apoptosis in A549 cells.

Several classic markers of apoptosis (Bax, Bcl-2, cleaved-caspase3 and cleaved-PARP) were detected by western blot analysis. The results demonstrated that BOS-93 could induce apoptosis via mitochondrial pathways. As presented in Fig. 3D, the expression levels of Bax were increased in BOS-93 treated cells, whereas expression levels of Bcl-2 were decreased. Furthermore, as the concentration of BOS-93 increased, the levels of cleaved caspase-3 and cleaved-PARP were increased (Fig. 3D).

BOS-93 induces autophagy in A549 cells. Following observing that BOS-93 induced apoptosis (Fig. 3A), it was determined that BOS-93 could induce autophagy in A549 cells. A549 cells were treated with BOS-93 for 48 h and evaluated by transmission electron microscopy. As presented in Fig. 4A, marked autophagic characteristics appeared in A549 cells following treatment with BOS-93. Autophagic vacuoles were detected by transmission electron microscopy. GFP-LC3 was used to detect the formation of autophagic vesicles. A549 cells were infected with recombinant adenoviral vector carrying GFP-tagged LC3, and then cells were examined under a fluorescence microscope. As presented in Fig. 4B, GFP-LC3 exhibited diffuse expression in untreated cells, whereas high punctate expression was observed in cells treated with BOS-93.

Another notable hallmark of autophagy is the conversion of LC3; specifically, the conversion of LC3-I (18 kDa) to LC3-II (16 kDa), which can be measured by western blot analysis (14). As presented in Fig. 4B, an increasing ratio of LC3-II/LC3-I was detected following treatment of BOS-93 for 48 h (Fig. 4C). Notably, the LC3-II/LC3-I ratio was decreased in the presence of the autophagy inhibitor, 3-MA (Fig. 4D).

Western blot analysis was used to examine the expression of autophagy-related proteins. As presented in Fig. 5A, the expressions of Atg14 and beclin-1 were increased in a concentration-dependent manner following treatment of BOS-93 for 48 h. Furthermore, the content of these proteins was decreased in the presence of 3-MA (Fig. 5B). These results indicated that A549 cells treated with BOS-93 were undergoing autophagy.

It has been reported that the PI3K/Akt/mTOR signaling pathway serves a major role in regulating autophagy in cancer cells (15). A549 cells were treated with BOS-93 (2.5, 5, and 10 μg/ml) for 48 h, and the associated proteins were analyzed using western blot analysis. As presented in Fig. 5C, treating A549 cells with BOS-93 for 48 h resulted in decreased phosphorylation of PI3k, Akt and mTOR.

BOS-93 stimulates ROS generation in A549 cells. The level of intracellular ROS was quantitatively estimated using a peroxide-sensitive fluorescent probe, DCFH-DA, and analyzed by flow cytometry. Compared with the control group, ROS was rapidly produced following exposure to A549 cells with BOS-93 (Fig. 6A and B). When treated with BOS-93 for 48 h, the mean DCF fluorescence in the 2.5, 5 and 10 μg/ml groups was increased by 279.38±71.23, 384.01±21.60 and 440.80±40.04%, respectively.

BOS-93 induces autophagy and apoptosis in A549 cells through ROS-dependent ERK and P38 MAPK activation. It has been reported that the activation of MAPKs, such as ERK and p38 MAPK, is associated with regulation of

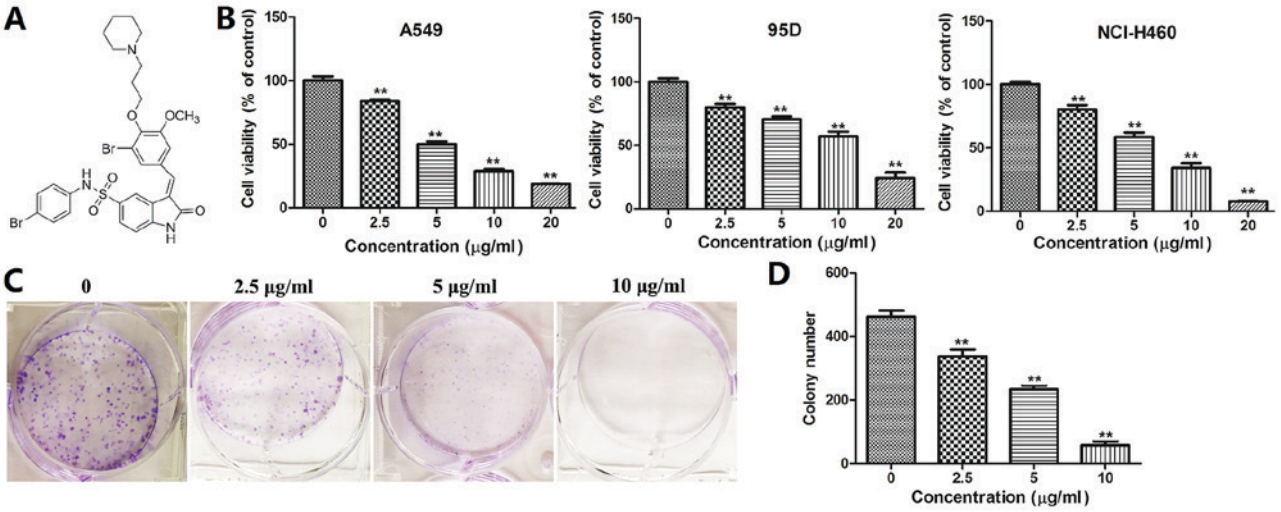

Figure 1. (A) Structure of BOS-93. (B) BOS-93 inhibits cell proliferation of A549 cells, 95D cells and NCI-H460 cells in a dose-dependent manner. Cell viability was evaluated by MTT assay. (C and D) BOS-93 inhibits colony formation of A549 cells. Data are expressed as mean + standard deviation (n=3). **P<0.01 vs. control group. BOS-93, 3-(3-bromo-5-methoxy-4-(3-(piperidin-1-yl)propoxy)benzylidene)-*N*-(4-bromophenyl)-2-oxoindoline-5-sulfonamide.

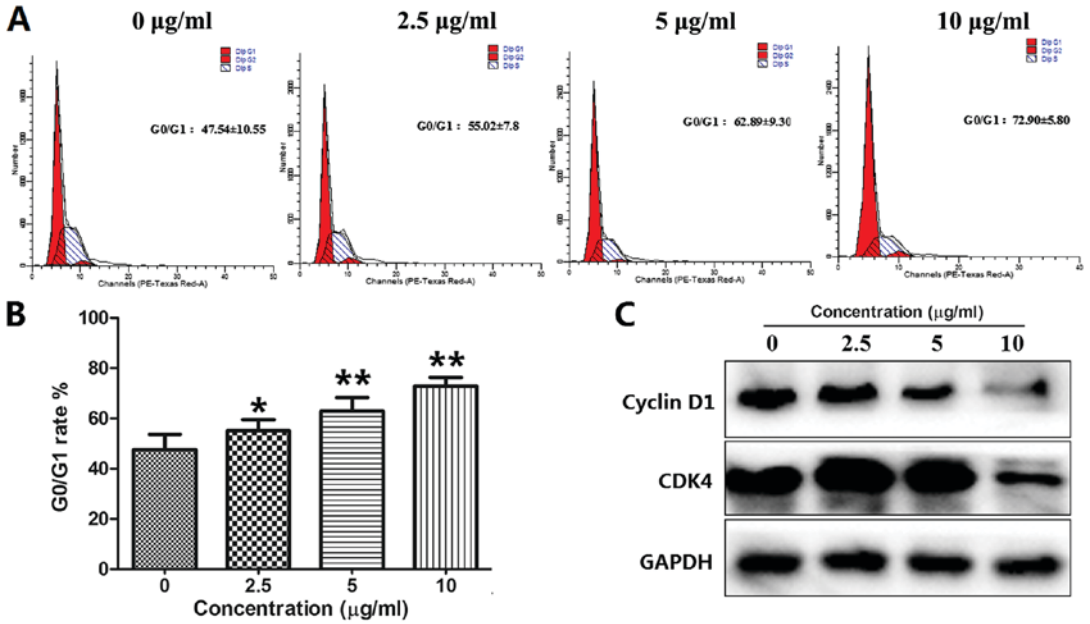

Figure 2. BOS-93 induces G0/G1 arrest. (A and B) A549 cells were treated with BOS-93 for 48 h and then harvested for cell cycle analysis by flow cytometry. (C) A549 cells were treated with BOS-93 for 48 h and then cell cycle-associated proteins, including cyclin D1 and CDK4 were analyzed using western blotting. Data are expressed as mean + standard deviation (n=3). *P<0.05, **P<0.01 vs. control group. BOS-93, 3-(3-bromo-5-methoxy-4-(3-(piperidin-1-yl)propoxy) benzylidene)-*N*-(4-bromophenyl)-2-oxoindoline-5-sulfonamide; CDK, cyclin-dependent kinase.

apoptosis and autophagy (15). A549 cells were treated with BOS-93 (2.5, 5, and 10 μg/ml) for 48 h, and the expression levels of ERK and p38 MAPK were analyzed by western blot analysis. As presented in Fig. 6C, following treatment of BOS-93, the phosphorylation of p-p38 and p-ERK was increased. These findings indicated that BOS-93 could induce apoptosis and autophagy in A549 cells via the ROS-mediated PI3K/Akt/mTOR and MAPK signaling pathways.

BOS-93 inhibits tumor growth in the in vivo A549 cell xenograft model. In order to evaluate the anti-tumor properties of BOS-93 *in vivo*, an A549 xenografted athymic mice mode was established in the present study. As presented in Fig. 7A, the tumor growth was markedly inhibited in the BOS-93 treated group at an inhibition ratio of 47.93%. Furthermore, there was no significant change in mice body weight during the experiment (Fig. 7B). For histological analysis, the heart, spleen and kidney were stained with hematoxylin and eosin, as presented in Fig. 7C, and there were no marked histological changes in these tissues following treatment with BOS-93, these results may suggest that the anti-tumor activity of BOS-93 has low toxicity on athymic mice.

It was further demonstrated that BOS-93 induced apoptosis and autophagy *in vivo*. Immunohistochemistry with Ki 67 (a cell proliferation marker) and LC3B (a cell autophagy marker) were examined in paraffin-embedded tumor sections. As

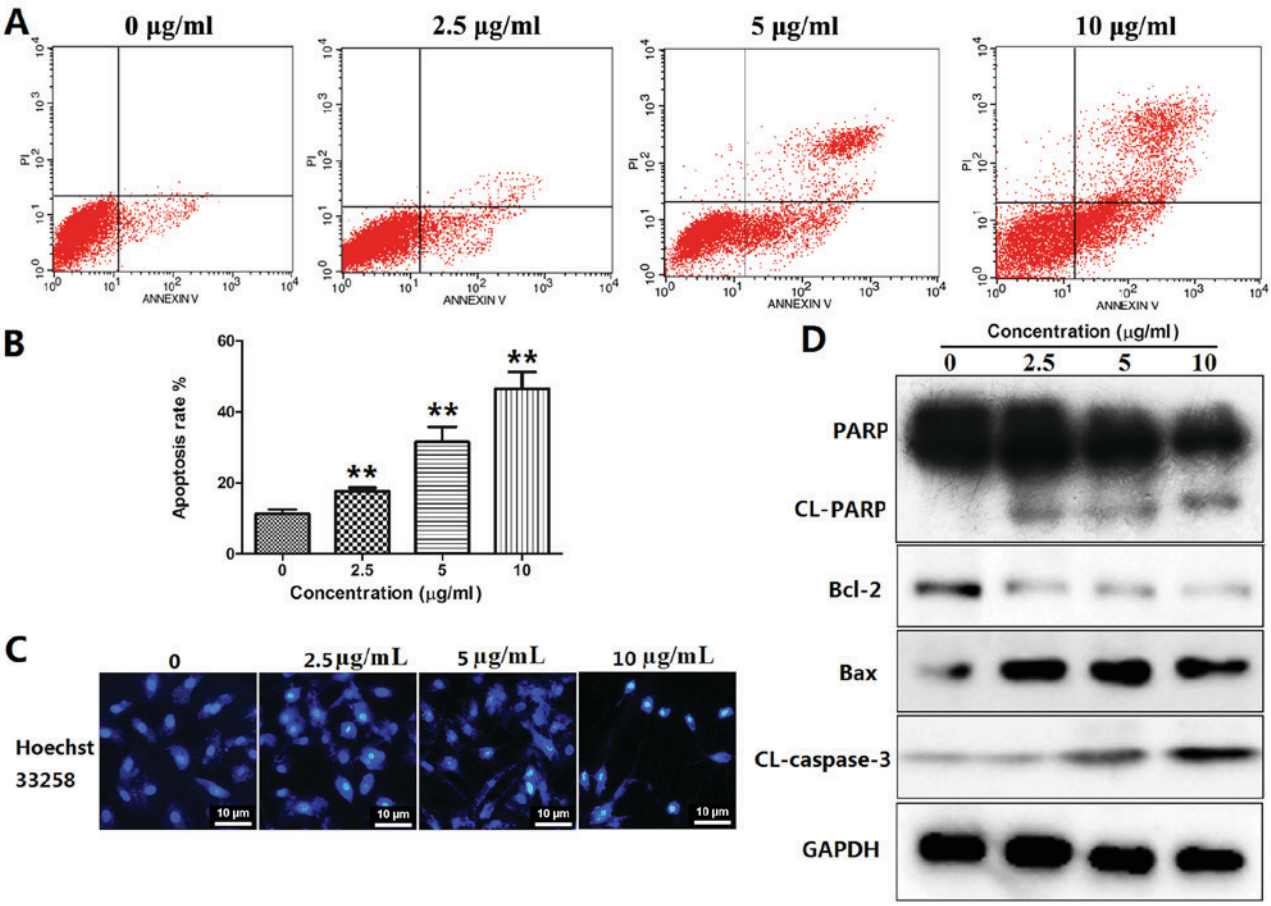

Figure 3. BOS-93 induces cell apoptosis. (A and B) A549 cells were treated with BOS-93 for 48 h, and then cells were stained with Annexin V/PI and analyzed by flow cytometry. (C) A549 cells were treated with BOS-93 for 48 h, and then cells were stained with Hoechst 33258 and photographed using fluorescence microscopy (scale bar, 50 μm). (D) A549 cells were treated with BOS-93 for 48 h and then apoptosis-associated proteins, including cleaved-PARP, Bcl-2, Bax and cleaved-caspase-3 were analyzed using western blotting. Data are expressed as mean + standard deviation (n=3). **P<0.01 vs. control group. BOS-93, 3-(3-bromo-5-methoxy-4-(3-(piperidin-1-yl)propoxy)benzylidene)-*N*-(4-bromophenyl)-2-oxoindoline-5-sulfonamide; PI, propidium iodide; PARP, poly ADP ribose polymerase; Bcl-2, B cell lymphoma-2; Bax, Bcl-2-associated X protein; CL, cleaved.

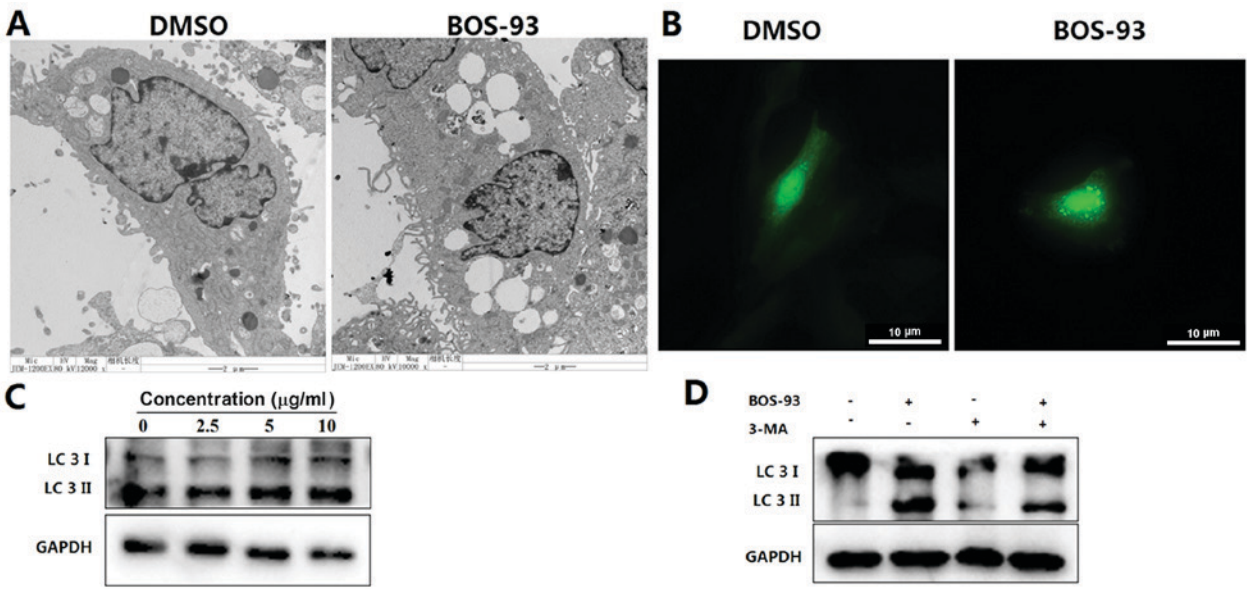

Figure 4. BOS-93 induces autophagy in A549 cells. (A) Transmission electron microscopy examination of morphology changes of A549 cells with or without BOS-93 (10 μg/ml) for 48 h. (B) A549 cells were infected with recombinant adenovirus expressing green fluorescent protein-LC3 and then cells were treated with 10 μg/ml BOS-93 for 48 h. (C) Western blot analysis of LC3 in A549 cells following incubation with or without BOS-93. (D) A549 cells were pretreated for 1 h in the presence or absence of 3-MA (5 mM) prior to addition of BOS-93. Western blot analysis of LC3 was performed following addition of 10 μg/ml BOS-93 for 48 h. BOS-93, 3-(3-bromo-5-methoxy-4-(3-(piperidin-1-yl)propoxy)benzylidene)-*N*-(4-bromophenyl)-2-oxoindoline-5-sulfonamide; LC3, light chain 3; DMSO, dimethyl sulfoxide.

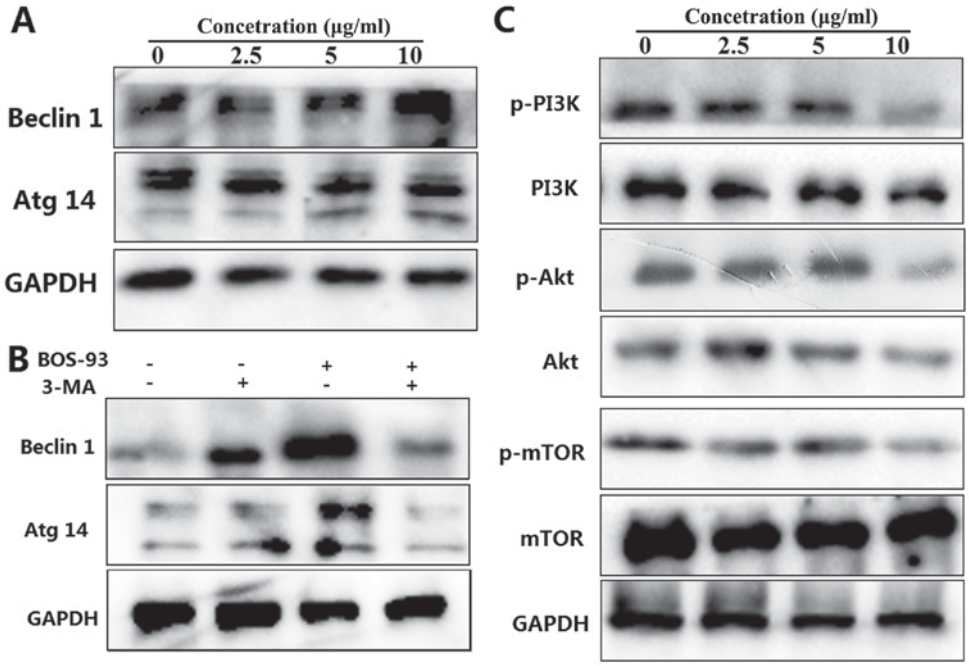

Figure 5. (A) Effects of BOS-93 on the levels of beclin-1 and Atg14 proteins. A549 cells were treated with BOS-93 for 48 h and then autophagy-related proteins, including beclin-1 and Atg14 were analyzed using western blotting. (B) A549 cells were pretreated for 1 h in the presence or absence of 3-MA (5 mM) prior to addition of BOS-93. Western blot analysis of beclin-1 and Atg14 was performed following addition of 10 μg/ml BOS-93 for 48 h. (C) A549 cells were treated with BOS-93 (0, 2.5, 5 or 10 μg/ml) for 48 h. The expressions of PI3K, Akt, mTOR, p-PI3K, p-Akt and p-mTOR were assessed by western blot analysis. GAPDH was used to normalize protein content. All data were representative of three independent experiments. BOS-93, 3-(3-bromo-5-methoxy-4-(3-(piperidin-1-yl)propoxy)benzylidene)-*N*-(4-bromophenyl)-2-oxoindoline-5-sulfonamide; Atg14, autophagy-related gene 14; PI3K, phosphoinositide 3-kinase; Akt, protein kinase B; mTOR, mechanistic target of rapamycin; p, phosphorylated.

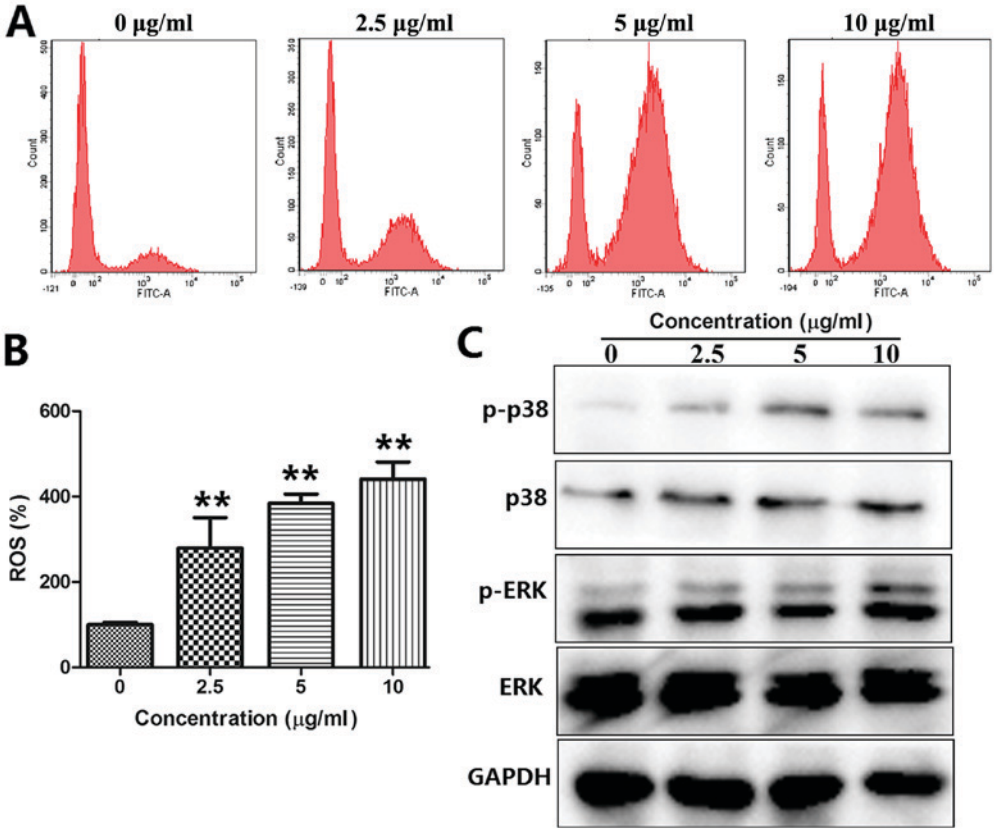

Figure 6. BOS-93 induces ROS generation. (A and B) A549 cells were treated with various concentrations of BOS-93 for 48 h and then cells were stained with 2',7'-dichlorofluorescein diacetate and analysis using flow cytometry. (C) A549 cells were treated with BOS-93 for 48 h and then the expressions of p38, ERK, p-p38 and p-ERK were analyzed using western blotting. Data are expressed as mean + standard deviation (n=3). **P<0.01 vs. control group. BOS-93, 3-(3-bromo-5-methoxy-4-(3-(piperidin-1-yl)propoxy)benzylidene)-*N*-(4-bromophenyl)-2-oxoindoline-5-sulfonamide; ROS, reactive oxygen species; ERK, extracellular signal-regulated kinase; p, phosphorylated.

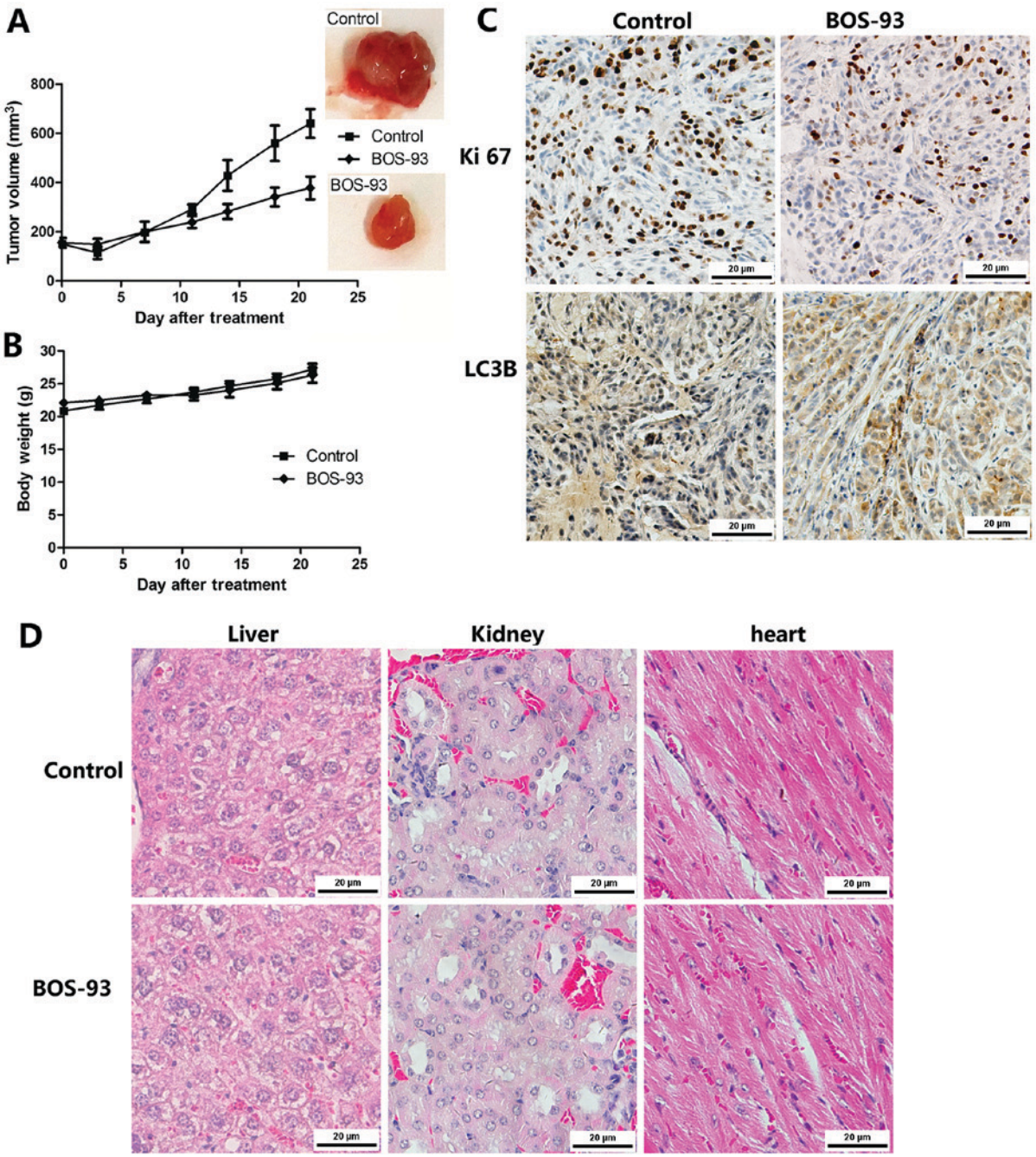

Figure 7. Effect of BOS-93 on tumor growth in A549-xenografted athymic mice. (A) BOS-93 was dissolved in 0.5% carboxymethyl cellulose-Na and administrated intraperitoneally once per day, tumor volume was recorded every 3 days until animals were sacrificed at day 21 (tumor images were taken on day 21). (B) The mean weights of treated and control mice were recorded every 3 days. (C) Immunohistochemistry for Ki 67 and LC3B were performed on paraffin-embedded tumor sections. (D) Organs from treated and control groups were stained with hematoxylin and eosin to evaluate the toxicity of BOS-93. Images were captured under x100 magnification. BOS-93, 3-(3-bromo-5-methoxy-4-(3-(piperidin-1-yl)propoxy)benzylidene)-*N*-(4-bromophenyl)-2-oxoindoline-5-sulfonamide; LC3, light chain 3.

presented in Fig. 7D, BOS-93 treatment markedly decreased the expression of Ki 67 and increased the expression of LC 3B compared with the control group.

Discussion

A novel bromophenol, BOS-93, was synthesized in the CAS Key Laboratory of Experimental Marine Biology, Institute of Oceanology, Chinese Academy of Sciences (6). In the present study, it was demonstrated that BOS-93 could lead to growth inhibition of human A549 lung cancer cells in association with apoptosis and autophagy. It was demonstrated that BOS-93 induced the loss of viability on human lung cancer cells, and the IC_{50} value on A549 cells was 4.78±0.56 μg/ml. The present results also indicated that BOS-93 could significantly inhibit colony formation in A549 cells. Furthermore, BOS-93 inhibited tumor growth without causing apparent toxicity effect in A549 cell xenograft model.

Regulation of cell growth and proliferation of mammalian cells are mediated through cell cycle progression (18). In the

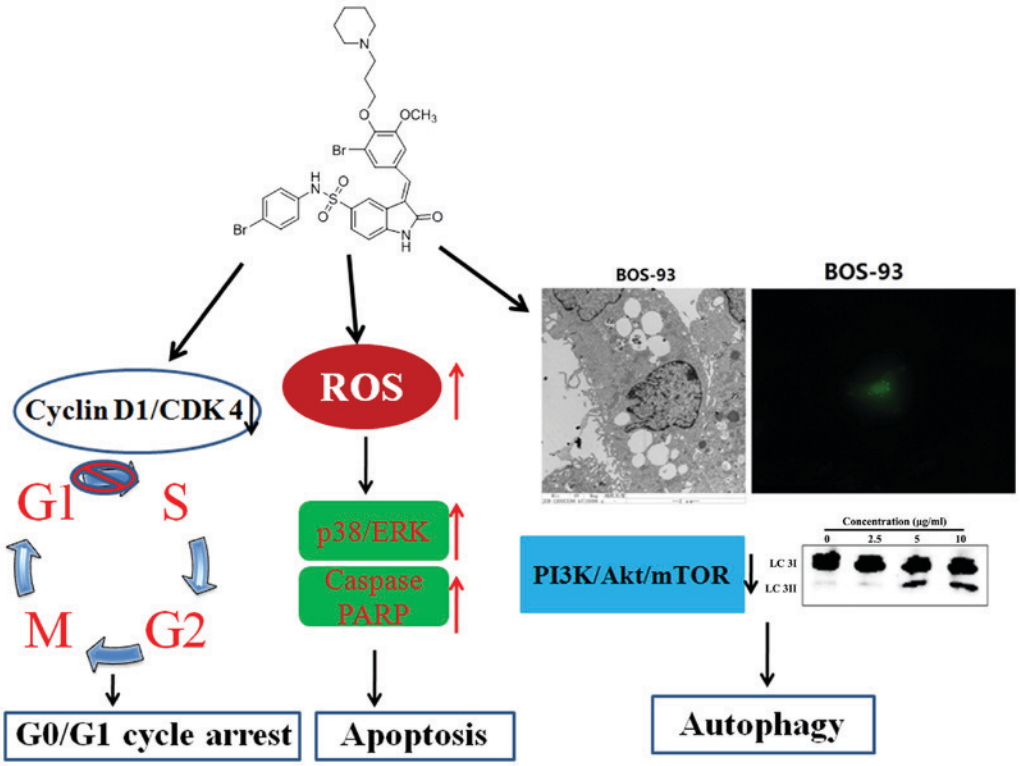

Figure 8. The proposed molecular mechanisms of apoptosis and autophagy induced by BOS-93 in A549 cells. BOS-93, 3-(3-bromo-5-methoxy-4-(3-(piperidin-1-yl)propoxy)benzylidene)-*N*-(4-bromophenyl)-2-oxoindoline-5-sulfonamide; CDK, cyclin-dependent kinase; ROS, reactive oxygen species; ERK, extracellular signal-regulated kinase; PARP, poly ADP ribose polymerase; PI3K, phosphoinositide 3-kinase; Akt, protein kinase B; mTOR, mechanistic target of rapamycin; LC3, light chain 3.

present study, cell cycle analysis demonstrated that BOS-93 could induce G0/G1 cell cycle arrest in A549 cells. It is well known that cyclin-dependent kinases serve an important role in cell cycle regulation (19). Additionally, BOS-93 induces G0/G1 cell cycle arrest by inhibiting the activity of cyclin-dependent kinases cyclin D1 and CDK 4 (20). The present study indicated that BOS-93 could exert its anti-proliferative effect via the modulation of cyclin-CDK machinery-mediated cell-cycle arrest.

Apoptosis serves a key role in the regulation of cells. It mainly comprised two apoptotic pathways: The death receptor-mediated apoptosis pathway and the mitochondria-mediated apoptosis pathway (21). In the latter, proteins from the Bcl-2 family, such as Bax and Bcl-2, are the main components that regulate mitochondrial permeability. The implementation of apoptosis is achieved through a proteolysis chain reaction comprising, for example, the caspase family (22). In the present study, it was demonstrated that BOS-93 treatment could increase the ratio of Bax/Bcl-2 as well as activate caspase-3 and PARP. These results indicated that BOS-93 could activate the mitochondrial apoptotic pathway in A549 cells. In addition, it has been reported that ROS serves a key role in the process of mitochondria-mediated apoptosis (23). In the present study, an increase in ROS generation was observed in cells treated with BOS-93, indicating that ROS serves an important role in BOS-93-induced apoptosis.

In research on chemotherapeutic drugs, apoptosis is commonly considered to be a prevailing anti-cancer mechanism (24-26). However, apoptosis is not the only such mechanism; other forms of cell death, such as autophagy, can also occur (27). When autophagy occurs, certain morphological characteristics, such as autophagosomes, can be observed by TEM (28). Notably, TEM also revealed that BOS-93 induces cell autophagy.

Microtubule-associated protein LC3 is a cytoplasmic protein that is quickly cleaved to form LC3-I (18 kDa) (29). It is activated by lipidation with phosphatidylethanolamine to form LC3-II (16 kDa), and the amount of LC3-II is correlated with the number of autophagosomes (29). The conversion of LC3-I (18 kDa) to LC3-II (16 kDa) typically corresponds to an increase in the rate of autophagy (28,30). In the present study, TEM was used to detect the effect of BOS-93 on the ultrastructure of A549 cells. Following BOS-93 treatment, the A549 cells displayed morphological characteristics associated with cell autophagy. Ad-GFP-LC3 was used to detect GFP-LC3 translocation in A549 cells. GFP-LC3 exhibited diffuse expression in untreated cells but high punctate expression in BOS-93-treated cells. Western blot analysis revealed accumulation of autophagosome-bound LC3-II. This phenomenon was reversed when cells were treated with 3-MA, an autophagy inhibitor, which indicated that BOS-93 induces autophagy of A549 cells.

It has been reported that the molecular machinery of autophagy is largely directed by a number of Atgs. For example, previous studies have demonstrated that Atg 14 and beclin-1 are essential for the formation of autophagosomal precursor (9,14). In the present study, the expression of Atg14 and beclin-1 were determined using western blot analysis. the data demonstrated that BOS-93 treatment induced upregulation of Atg14 and beclin1. Furthermore, combining 3-MA with BOS-93 resulted in a significant decrease in the expression of

Atg14 and beclin-1 compared with BOS-93 cultured alone, suggesting that BOS-93 induced autophagy in A549 cells.

Given that both apoptosis and autophagy could be induced by BOS-93 in A549 cells, their mutual association was investigated. Several studies have reported that chemotherapeutic drugs can induce both apoptosis and autophagy in cancer cells (10,17). Autophagosome formation is regulated by the mTOR pathway, a major nutrient sensor (9). The present study demonstrated that, upon BOS-93 treatment, PI3K, Akt and mTOR phosphorylation was reduced in A549 cells, indicating downregulation of the PI3K/Akt/mTOR pathway.

MAPK signal pathways (including p38 MAPK and ERK1/2) are associated with the transduction of extracellular stimuli signals into cells and their nuclei and initiation of cellular biological reactions such as cell proliferation, differentiation, transformation and apoptosis (31,32). ROS can act as a second messenger to activate the MAPK signaling pathway (23). In addition, it is well known that p38 is closely associated with the initiation of apoptosis and the cell cycle (33). ERK1/2 is mainly activated by phosphorylation of various growth factors and oxidative stress, and it is closely associated with cell proliferation and differentiation (34). In the present study, it was demonstrated that BOS-93 treatment triggered ROS generation and increased phosphorylation of p38 and ERK, suggesting that the p38/ERK signaling pathway was associated with BOS-93 induced apoptosis and autophagy in A549 cells.

In conclusion, the present study demonstrated that BOS-93 could induce G0/G1 arrest, apoptosis and autophagy in A549 cells, and that BOS-93 could inhibit PI3K/Akt/mTOR and activate the MAPK pathway (Fig. 8). Furthermore, BOS-93 could also exert anti-tumor activity *in vivo*. Therefore, the findings indicated that BOS-93 may display excellent effects on human lung cancer cells and act as a multi-target anti-cancer drug due to its ability of leading to apoptosis and autophagy.

Acknowledgements

Not applicable.

Funding

The present study was supported by the National Natural Science Foundation of China (grant nos. 81773586 and 81703354) and Key Research Program of Frontier Sciences, CAS (grant no. QYZDB-SSW-DQC014), and the Project of Discovery, Evaluation and Transformation of Active Natural Compounds, Strategic Biological Resources Service Network Programme of Chinese Academy of Sciences (grant no. ZSTH-026), and Shandong Provincial Natural Science Foundation for Distinguished Young Scholars (grant no. JQ201722), and the National Program for Support of Top-notch Young Professionals, and Taishan Scholar Youth Project of Shandong Province.

Availability of data and materials

All data generated or analyzed during this study are included in this published article.

Authors' contributions

CG, LW and DS conceived and designed the present study. CG, LW, YZ, BJ and JL performed the experiments. CG and LW analyzed experimental data. CG wrote and revised the paper. All authors reviewed the manuscript.

Ethics approval and consent to participate

All studies in mice were approved by Institute of Oceanology, Chinese Academy of Sciences Laboratory Animal Care and Ethics Committee in accordance with the animal care and use guidelines.

Patient consent for publication

Not applicable.

Competing interests

The authors declare that they have no competing interests.

References

1. Blunt JW, Copp BR, Hu WP, Munro MH, Northcote PT and Prinsep MR: Marine natural products. Nat Prod Rep 24: 31-86, 2007.
2. Wang BG, Gloer JB, Ji NY and Zhao JC: Halogenated organic molecules of Rhodomelaceae origin: Chemistry and biology. Chem Rev 113: 3632-3685, 2013.
3. Liu M, Hansen PE and Lin XK: Bromophenols in marine algae and their bioactivities. Marine Drugs 9: 1273-1292, 2011.
4. Oztaskin N, Cetinkaya Y, Taslimi P, Göksu S and Gülçin I: Antioxidant and acetylcholinesterase inhibition properties of novel bromophenol derivatives. Bioorg Chem 60: 49-57, 2015.
5. Shi D, Guo S, Jiang B, Guo C, Wang T, Zhang L and Li J: HPN, a synthetic analogue of bromophenol from red alga Rhodomela confervoides: Synthesis and anti-diabetic effects in C57BL/KsJ-db/db mice. Mar Drugs 11: 350-362, 2013.
6. Wang LJ, Guo CL, Li XQ, Wang SY, Jiang B, Zhao Y, Luo J, Xu K, Liu H, Guo SJ, *et al*: Discovery of novel bromophenol hybrids as potential anticancer agents through the Ros-mediated apoptotic pathway: Design, synthesis and biological evaluation. Mar Drugs 15: pii: E343, 2017.
7. Hanahan D and Weinberg RA: Hallmarks of cancer: The next generation. Cell 144: 646-674, 2011.
8. Suzuki M, Endo M, Shinohara F, Echigo S and Rikiishi H: Rapamycin suppresses ROS-dependent apoptosis caused by selenomethionine in A549 lung carcinoma cells. Cancer Chemother Pharmacol 67: 1129-1136, 2011.
9. Lalaoui N, Lindqvist LM, Sandow JJ and Ekert PG: The molecular relationships between apoptosis, autophagy and necroptosis. Semin Cell Dev Biol 39: 63-69, 2015.
10. Kumar D, Shankar S and Srivastava RK: Rottlerin induces autophagy and apoptosis in prostate cancer stem cells via PI3K/Akt/mTOR signaling pathway. Cancer Lett 343: 179-189, 2014.
11. Duan P, Hu C, Quan C, Yu T, Zhou W, Yuan M, Shi Y and Yang K: 4-Nonylphenol induces apoptosis, autophagy and necrosis in Sertoli cells: Involvement of ROS-mediated AMPK/AKT-mTOR and JNK pathways. Toxicology 341: 28-40, 2016.
12. Kliosnky D, Abdelmohsen K, Abe A, Abedin MJ, Abeliovich H, Acevedo Arozena A, Adachi H, Adams CM, Adams PD, Adeli K, *et al*: Guidelines for the use and interpretation of assays for monitoring autophagy (3rd edition). Autophagy 12: 1-222, 2016.
13. Russell RC, Yuan HX and Guan KL: Autophagy regulation by nutrient signaling. Cell Res 24: 42-57, 2014.
14. Wu JJ, Yang C, Guo C, Li X, Yang N, Zhao L, Hang H, Liu S, Chu P, Sun Z, *et al*: SZC015, a synthetic oleanolic acid derivative, induces both apoptosis and autophagy in MCF-7 breast cancer cells. Chem Biol Interact 244: 94-104, 2016.

15. Shinojima N, Yokoyama T, Kondo Y and Kondo S: Roles of the Akt/mTOR/p70S6K and ERK1/2 signaling pathways in curcumin-induced autophagy. Autophagy 3: 635-637, 2007.
16. Jiang Y, Wang X and Hu D: Furanodienone induces G0/G1 arrest and causes apoptosis via the ROS/MAPKs-mediated caspase-dependent pathway in human colorectal cancer cells: A study in vitro and in vivo. Cell Death Dis 8: e2815, 2017.
17. Xie ZZ, Li MM, Deng PF, Wang S, Wang L, Lu XP, Hu LB, Chen Z, Jie HY, Wang YF, *et al*: Paris saponin-induced autophagy promotes breast cancer cell apoptosis via the Akt/mTOR signaling pathway. Chem Biol Interact 264: 1-9, 2017.
18. Wang R, Zhang Q, Peng X, Zhou C, Zhong Y, Chen X, Qiu Y, Jin M, Gong M and Kong D: Stellettin B induces G1 arrest, apoptosis and autophagy in human non-small cell lung cancer A549 cells via blocking PI3K/Akt/mTOR pathway. Sci Rep 6: 27071, 2016.
19. Gupta S: Molecular steps of death receptor and mitochondrial pathways of apoptosis. Life Sci 69: 2957-2964, 2001.
20. Guo CL, Wang LJ, Zhao Y, Liu H, Li XQ, Jiang B, Luo J, Guo SJ, Wu N and Shi DY: A novel bromophenol derivative BOS-102 induces cell cycle arrest and apoptosis in human A549 lung cancer cells via ROS-mediated PI3K/Akt and the MAPK signaling pathway. Mar Drugs 16: pii: E43, 2018.
21. Wu CC and Bratton SB: Regulation of the intrinsic apoptosis pathway by reactive oxygen species. Antioxid Redox Signal 19: 546-558, 2013.
22. Adams JM and Cory S: The Bcl-2 apoptotic switch in cancer development and therapy. Oncogene 26: 1324-1337, 2007.
23. Liu J, Chang F, Li F, Fu H, Wang J, Zhang S, Zhao J and Yin D: Palmitate promotes autophagy and apoptosis through ROS-dependent JNK and p38 MAPK. Biochem Biophys Res Commun 463: 262-267, 2015.
24. Kim R, Emi M, Tanabe K, Uchida Y and Toge T: The role of fas ligand and transforming growth factor beta in tumor progression: Molecular mechanisms of immune privilege via Fas-mediated apoptosis and potential targets for cancer therapy. Cancer 100: 2281-2291, 2004.
25. Hassan M, Watari H, AbuAlmaaty A, Ohba Y and Sakuragi N: Apoptosis and molecular targeting therapy in cancer. Biomed Res Int 2014: 150845, 2014.
26. Burz C, Berindan-Neagoe I, Balacescu O and Irimie A: Apoptosis in cancer: Key molecular signaling pathways and therapy targets. Acta Oncol 48: 811-821, 2009.
27. Okada H and Mak TW: Pathways of apoptotic and non-apoptotic death in tumour cells. Nat Rev Cancer 4: 592-603, 2004.
28. Lockshin RA and Zakeri Z: Apoptosis, autophagy, and more. Int J Biochem Cell Biol 36: 2405-2419, 2004.
29. Kuma A, Matsui M and Mizushima N: LC3, an autophagosome marker, can be incorporated into protein aggregates independent of autophagy: Caution in the interpretation of LC3 localization. Autophagy 3: 323-328, 2007.
30. Chen SD, Wu CL, Hwang WC and Yang DI: More insight into BDNF against neurodegeneration: Anti-apoptosis, Anti-oxidation, and suppression of autophagy. Int J Mol Sci 18: pii: E545, 2017.
31. Ki YW, Park JH, Lee JE, Shin IC and Koh HC: JNK and p38 MAPK regulate oxidative stress and the inflammatory response in chlorpyrifos-induced apoptosis. Toxicol Lett 218: 235-245, 2013.
32. Fang H, Cong L, Zhi Y, Xu H, Jia X and Peng S: T-2 toxin inhibits murine ES cells cardiac differentiation and mitochondrial biogenesis by ROS and p-38 MAPK-mediated pathway. Toxicol Lett 258: 259-266, 2016.
33. Bulavin DV, Phillips C, Nannenga B, Timofeev O, Donehower LA, Anderson CW, Appella E and Fornace AJ Jr: Inactivation of the Wip1 phosphatase inhibits mammary tumorigenesis through p38 MAPK-mediated activation of the p16(Ink4a)-p19(Arf) pathway. Nat Genet 36: 343-350, 2004.
34. Yoon S and Seger R: The extracellular signal-regulated kinase: Multiple substrates regulate diverse cellular functions. Growth Factors 24: 21-44, 2006.